27th ABCM International Congress of Mechanical Engineering
December 04-08, 2023, Florianópolis-SC, Brazil

COB-2023-1233
INVESTIGATION OF SWIRLING FLOW EFFECT ON AN AXIAL COMPRESSOR PARAMETERS VIA CFD

Patrick Donegá Queiroz
Institute for Technological Research, São Paulo, Brazil
patrickqueiroz@ipt.br

André Damiani Rocha
Federal University of ABC, São Paulo, Brazil
a.damiani@ufabc.edu.br

André Mitsuo Kogishi
Institute for Technological Research, São Paulo, Brazil
amkogishi@ipt.br

João Lucas Dozzi Dantas
Hydro and Aerodynamics Department, FORCE Technology, Kongens Lyngby, 2800, Copenhagen, Denmark
joda@forcetechnology.com

Abstract. *Compressors are a type of turbomachinery used to increase the pressure of a fluid. Among them, axial compressors possess high mass flow, which benefits many applications, such as gas turbines in aeronautic engines that require a significant amount of air in the combustion chamber to burn the fuel. Inlet Guide Vanes (IGVs) are utilized to enhance the performance and broaden the operational range of axial compressors by applying pre-swirl to the incoming flow, reducing the Mach number through a reduction in resultant relative velocity. The objective of this study is to investigate an axial compressor with an IGV stage and its influence on the compressor performance parameters using CFD based models. A base model with one IGV blade angle was compared/validated against experimental data to ensure the model prediction capabilities in the IGV blade investigation, whereas the blade angles were changed several times to cover all conditions. The results revealed that increasing the IGV angle led to a decrease in compression ratio; however, efficiency improved, peaking at 15º, where the isentropic efficiency was 84.5%, a 5% improvement. However, at higher angles, the formation of vortices caused a decrease in efficiency.*

Keywords: *Axial compressors; Aeronautic Engines; Inlet Guide Vanes; Computational Fluid Dynamics; Efficiency*

1. INTRODUCTION

Turbomachinery exchanges energy with a working fluid through the rotation of a shaft. Specifically, compressors are turbomachinery that have the role of increasing the pressure of a working fluid. An axial compressor is one in which the flow of the working fluid occurs along the axis and is typically used in applications that require large mass flows, such as gas turbines, used for various applications, including aero engines that provide propulsion to aircraft and in the energy industry for power generation, among other industrial applications (Farokhi, 2014). Particularly, in aeronautic engine applications, gas turbines account for at least 50% of the value of an aircraft.

Since the conception of gas turbines, efforts have been made to improve the operating conditions and parameters. One of the solutions used for over 70 years are the Inlet Guide Vanes (IGV), which consists of a set of stationary blades upstream of the compressor air inlet, applying a swirl to the incoming flow. This allows the compressor to operate with higher efficiency and further away from the stall condition. When properly designed, it enables emission reduction, reduced fuel consumption, and increased engine life and reliability (Vlady et al., 2021). The latest aeronautical engines, turbofans, have a set of IGV blades upstream of the fans, at the entrance to the engine core (compressor + combustion chamber + turbine), and a variation in the bypass section (the admitted air that does not participate in the combustion but flows around the core and mixes with the combustion gases), called Outlet Guide Vanes (OGVs) (Daroukh, 2017).

Methods for amplifying efficiency are still widely studied, and, with the facilitation of access to numerical methods, such as CFD, and high-speed clusters, the investigation of many possibilities and its variations have become very common. Solutions as serpentine ducts, that also applies a swirl to the incoming flow, were investigated through numerical methods (Fredrick, 2010). In the works of Matteo (2013), Frohnapfel (2019), Kozak (2000), Singh and Kaurase (2016), Vlady et al. (2021), among others, IGV and its influence on gas turbines were studied, with the support of experimental and numerical methods, on many different scenarios and configurations, such as flow control (Kozak, 2000), different climate (Singh and Kaurase, 2016), with variable IGV blade angle (Vlady et al., 2021), etc. Each of these works, and others, contributed to expand the current knowledge on how to operate gas turbines more efficiently and use the phenomenon of swirling flow in our favor. Additionally, the use of numerical methods contribute for building a methodology of simulation that is adequate for cases likes this and allow a broader study of these machines and perform methods of optimization.

The present work aims to study axial compressors with a set of IGV blades and, through a CFD numerical model, observe how the variation of the IGV blade angle affects the operational parameters of the compressor. With the results obtained a deeper understanding of axial compressors will be attained and the validated numerical model, built through the process, can be helpful for future works. Other than that, is expected from this work a validation of the use of IGVs on axial compressors and its positive effect on operational parameters.

1.1 AXIAL COMPRESSORS

A set of rotor blades followed by a set of stator blades is called a stage. An isolated axial stage is capable of a high mass flow rate; however, it has a low compression ratio, typically between 1.5 and 2, so an axial compressor is composed of a sequence of stages to achieve the required total compression for the application. The set of rotor blades has the role of transferring energy to the working fluid, while the set of stator blades reduces the flow velocity, increases the static pressure, and balances the stage output (Matteo, 2013).

The main parameters used in the analysis of compressors are the pressure ratio (π_p), temperature ratio (π_t), and the isentropic efficiency of the stage (η). The isentropic efficiency relates the compression of the actual process to an ideal (adiabatic) compression, where there is no heat exchange with the surroundings or other losses (Matteo, 2013). These parameters are presented in Eq. (1), Eq. (2) and Eq. (3), respectively.

$$\pi_C = \frac{P_{out}}{P_{in}}, \tag{1}$$

$$\pi_T = \frac{T_{out}}{T_{in}} \ , \tag{2}$$

$$\eta = \frac{\pi_C^{\left[\frac{\gamma}{\gamma-1}\right]} - 1}{\pi_T - 1}, \tag{3}$$

In Eq. (1), Eq. (2) and Eq. (3), P_{in} is the inlet total pressure, P_{out} is the stage outlet total pressure, T_{in} is the inlet total temperature, T_{out} is the outlet total temperature and γ is the ratio of molar specific heats at constant pressure (C_p) and constant volume (C_v).

In its original form, isentropic efficiency relates the inlet and outlet total enthalpies measured in the real case to the ideal case, but measuring enthalpies is more complicated compared to measuring pressures and temperatures.

1.2 INLET GUIDE VANES (IGVs)

One of the structures developed to modify the operating parameters of axial compressors are the Inlet Guide Vanes (IGVs). Structures of this type, which have a mechanism to change the angle of their blades, are called Variable Inlet Guide Vanes (VIGV). Their function is to apply a swirl to the compressor's incoming flow. The swirl is the tangential component of the working fluid's absolute velocity that is parallel to the tangential velocity of the blade. The variation of swirl caused by the IGVs is known and will be referred to in this work as pre-swirl, which is defined as positive when in the same direction as the compressor rotation (Vlady et al., 2021). Figure 1 shows the velocity triangle for a compressor with a set of IGVs and a stage.

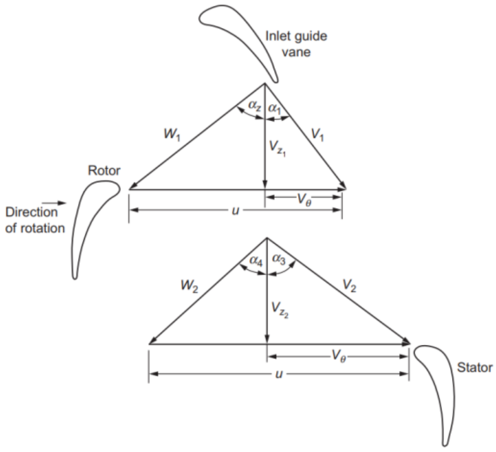

Figure 1. Axial Compressor Velocities Triangle. (SOURCE: Boyce, 2012)

In general, the air enters with absolute velocity (V_1) at an angle (α_1), which can be decomposed into axial velocity (V_{Z1}) and tangential velocity ($V_{\theta 1}$). When vectorially combined with the tangential velocity of the compressor blades (U), it produces the resulting relative velocity (W_1) at an angle (α_2). After passing through the rotor set, the resulting relative velocity becomes (W_2) at an angle (α_4). The aerodynamic profile causes the angle (α_4) to be smaller than (α_2) due to the curvature and (W_2) to be smaller than (W_1) due to the trailing edge being slimmer than the leading edge, increasing the passage area and causing diffusion. When vectorially combined, (W_2) with the rotor blade velocity determines the absolute velocity of the air (V_2) at the inlet of the stator blades. The angle (α_1) can be controlled by the IGV angle. In the case where this angle is 0° (or IGVs are absent), the tangential component of the absolute velocity of the air at the inlet ($V_{\theta 1}$) will not exist. When a positive swirl is applied, an increase in the angle (α_1) causes a decrease in the angle (α_2), and since the rotor blade speed remains unchanged, the component (W_1) is reduced. Considering the non-zero pre-swirl, the Euler equation for the rotor takes the form of Eq. (4), where H is the total enthalpy rise and g is the gravity (Boyce, 2012).

$$H = \frac{1}{g} * [U_1 * V_{\theta 1} - U_2 * V_{\theta 2}], \tag{4}$$

Knowing that the set of rotor blades have the same velocity at the inlet and outlet, it is possible, through the relationships $V_{\theta 1} = V_{z1}*\tan(\alpha_1)$ and $V_{\theta 2} = V_{z2}*\tan(\alpha_3)$, and if the axial velocity remains unchanged in the rotor stage, to rewrite Eq. (4) as Eq. (5).

$$H = \frac{U*V_z}{g} * [\tan(\alpha_1) - \tan(\alpha_3)], \tag{5}$$

Eq. (5) is expressed in terms of the absolute velocities at the inlet and outlet of the stage. By rewriting it in terms of the relative angles of the airflow, Eq. (6) is obtained.

$$H = \frac{U*V_z}{g} * [\tan(\alpha_2) - \tan(\alpha_4)], \tag{6}$$

Furthermore, assuming ideal gas, Eq. (6) can be written to calculate the pressure rise in the stage, given by Eq. (7).

$$\frac{P_2}{P_1} = \left[\frac{U*V_z}{g*C_p*T_{in}} * [\tan(\alpha_2) - \tan(\alpha_4)] + 1\right]^{\frac{\gamma}{\gamma+1}}, \tag{7}$$

From Eq. (6), it can be observed that in the case of positive pre-swirl, the work produced by the rotor is lower. This is because the difference between the relative angles is reduced, which, when transferred to Eq. (7), results in a lower compression ratio. On the other hand, negative pre-swirl increases the compression ratio (Boyce, 2012).

Additionally, the relative Mach number at the rotor inlet is given by Eq. (8). In this equation, the Mach number (M) is calculated as the ratio of the resulting relative velocity (W_1) to the speed of sound (a_1).

$$M_{rel} = \frac{W_1}{a_1}, \tag{8}$$

Since the resulting relative velocity (W_1) is reduced and the speed of sound (a_1) remains unchanged, positive pre-swirl reduces the Mach number at the rotor inlet. This is the primary effect that motivates the installation of a set of IGV blades, because as W_1 gets closer to the sonic condition or as the Mach number increases in the supersonic regime, compressive effects such as shock waves and increased air density occur more intensely, as well as the blockage effect, resulting in greater losses. Therefore, lower Mach numbers at the inlet are reflected in higher compressor efficiencies (Boyce, 2012).

Figure 2 shows efficiency curves as a function of the pre-swirl angle at the inlet and demonstrates a limit to this efficiency increase, reaching a point where it begins to decrease again (Boyce, 2012). This decrease in efficiency occurs because, beyond a certain point, at a given blade inclination, a turbulent wake will start to develop more intensely from the leading edge, creating many more sources of losses in the internal flow of the compressor (Frank et al., 2021).

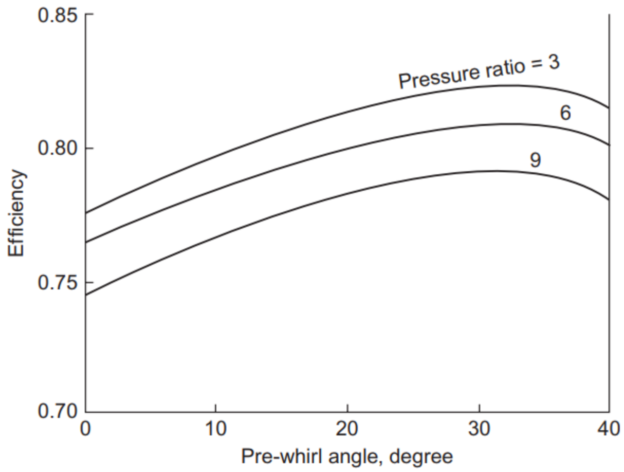

Figure 2. Swirl angle effect on compressor efficiency. (SOURCE: Boyce, 2012)

2. NUMERIC MODEL

2.1 MODEL SETTINGS

The model of an axial compressor was built using the tools from the commercial ANSYS® package, and the modules used are explained below.

The model consists of 3 sets of blades: IGV, rotor, and stator. The rotor and stator blades from Stage 37 were used, which is an experimental stage developed by NASA and extensively used for research, with available experimental data (NASA, 1978). Therefore, it has known parameters and geometry, and its geometry files are available.

The rotor set has 36 blades, while the stator set has 46 blades. For the construction of the IGV set, slender flat plates were used, also with 36 blades. This profile is not the most efficient for this application, but it allows for greater flexibility in modifications and enables the observation of the desired effects.

2.1.1 BLADES GEOMETRY

The ANSYS BladeGen® was used to model the geometry of the IGV blades, shroud, and hub. The swirling flow is generated by tilting the blades, regenerating the geometry multiple times. In Figure 3, the geometry of the blades aligned with the flow is presented.

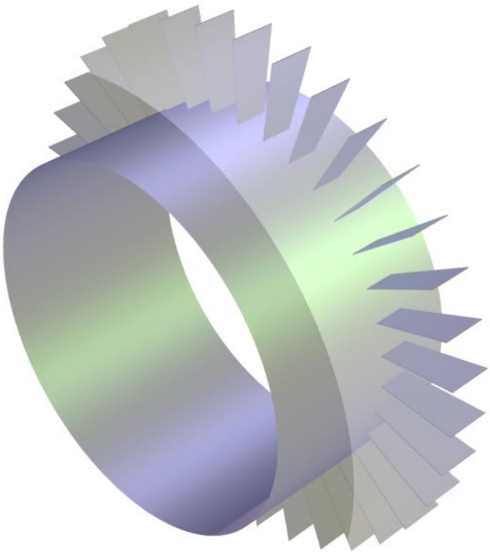

Figure 3. IGV blades with 0º deflection.

2.1.2 MESH GENERATION

The ANSYS TurboGrid® was used to generate a hexahedral mesh for the fluid around the blades. Figure 4 shows the mesh for the geometry presented in Figure 3, also showing the boundary conditions applied in the geometry surfaces: IGV blade, hub, shroud, inlet, outlet, and periodic surfaces.

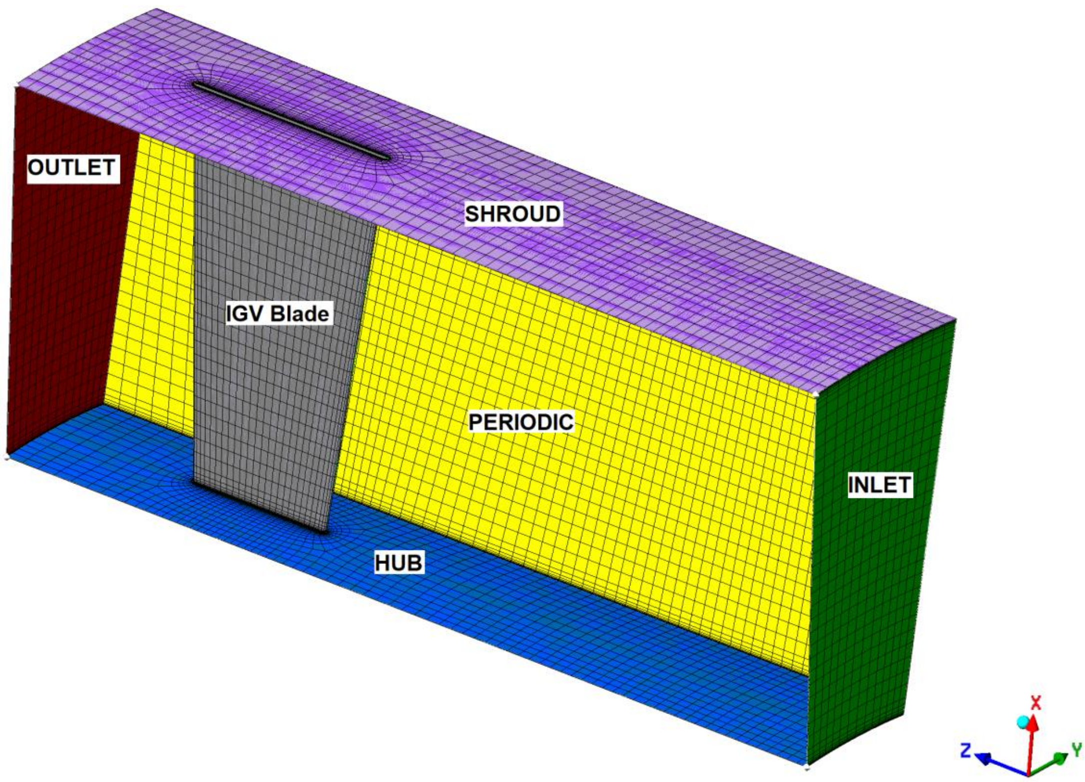

Figure 4. Generated mesh to the IGV blades with 0º deflection.

The periodic surface is crucial because it is where the geometry will be radially replicated, allowing the simulation of only one blade from each set and considerably reducing the simulation time.

2.1.3 CFD MODEL

The CFD model was developed using the ANSYS CFX software, which is suitable for turbomachinery applications. Figure 5 shows the domain assembly in the simulation module.

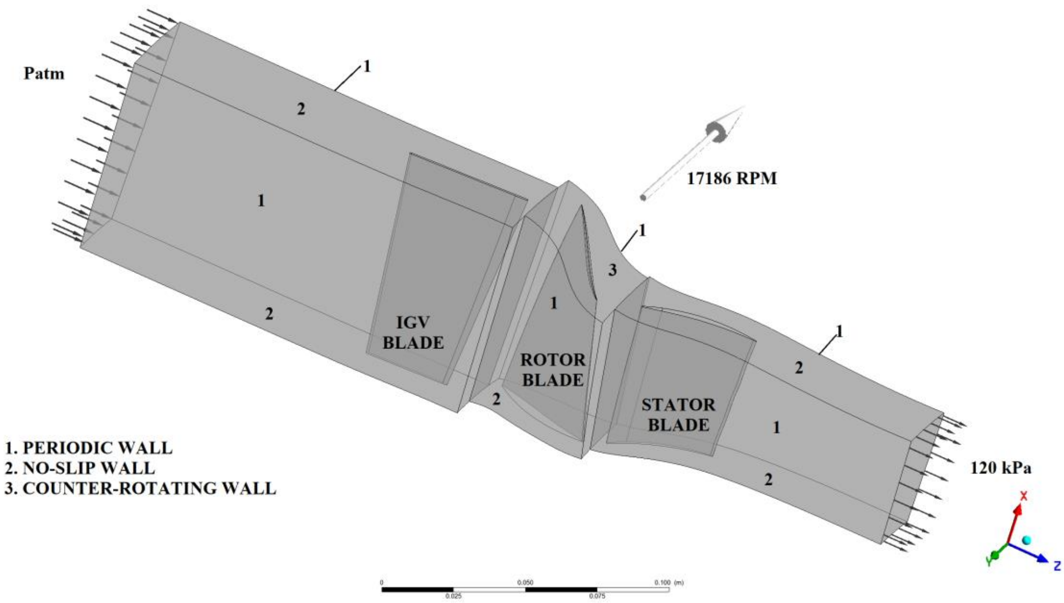

Figure 5. ANSYS CFX simulation setup.

To reproduce the experimental results numerically, the model was set up with the parameters defined and measured in the test (NASA, 1978): a rotation speed of 17186 RPM, an inlet at atmospheric pressure, and an outlet with a fixed total pressure of 120 kPa. The periodicity conditions were applied to the side walls as mentioned. The walls of the stationary blade, hub, and shroud sets are 'no slip' walls, while the rotor shroud wall is counter-rotating, simulating the effect of stage rotation.

The simulations were performed over 1000 iterations using the steady state model, using air modeled as an ideal gas without buoyancy modeling. A heat transfer model by total energy was applied, without combustion or radiation terms. According to Simões et al., 2009, the most suitable turbulence model for this case is k-ω with Shear Stress Transport (SST) model, eliminating the need to study various turbulence models. The advection and turbulence schemes are set to use second order terms. The temporal scale control is automatic with a factor of 1 and a conservative length scale option. The convergence criterion is RMS, with residuals of 10^-6.

2.2 VALIDATION AND MESH INDEPENDENCE STUDY

The validation was performed in order to ensure that the model is suitable for reproducing the test conditions. For this purpose, the CFD model results were compared with experimental data obtained from NASA files, which are publicly available for consultation (NASA, 1978). Stage 37 was originally tested in various configurations without the presence of IGVs. The case described in the previous section was chosen, reproduced in the model, and are presented in Table 1, along with the simulation results pressure ratio (Pr), air mass flow rate ($\dot{m}$), and compressor efficiency (η).

Table 1. Results from the Stage 37 experiment (NASA, 1978) used for the validation of the developed model and simulation results for comparison.

Case	Pr	$\dot{m}$ [kg/s]	η [%]
Experimental Data	1.753	20.82	81.4
Simulation without IGVs	1.761	20.96	80.8
Simulation with IGVs (0,57 mi elements)	1.775	20.78	80.3
Simulation with IGVs (1,15 mi elements)	1.772	20.78	80.4

Initially, the simulation was performed to replicate the experimental setup without the presence of IGVs. Then, the set of IGV blades with a 0° angle of attack, meaning the chord aligned with the flow, was added. The model without the presence of IGVs achieved convergent results with small deviations compared to the experimental data, which is common for numerical models due to numerical errors or the inability to perfectly replicate all test conditions. However, the model meets the requirements of this work.

There is a slight influence of the symmetric IGVs on the results. In this case, the variation is not significant, which is expected because the symmetric nature of the IGV blades and their alignment with the flow make the conditions very similar to the base case.

A mesh independence study was conducted for the case with the presence of IGVs. Starting from the mesh used in the validation, which had 570,000 elements, a mesh with 1.15 million elements was created. When comparing the results between the 570,000-element mesh and the 1.15 million-element mesh, a high degree of similarity was observed, indicating that mesh refinement is unnecessary as it only represents a considerable increase in computational cost with minimal change in results. Taking all of this into consideration, meshes with similar refinement to the base case were used throughout the entire process.

3. RESULTS

To extract the results, the case was replicated multiple times, only varying the angle of the IGV blades. The angle started from the base case with IGV at 0° and was increased by 5°. Table 2, Figure 6 and Figure 7 present the obtained results.

Table 2. Results obtained from CFD simulations.

αIGV [°]	**0**	**5**	**10**	**15**	**20**
Pr	1.78	1.74	1.70	1.66	1.62
η [%]	80.50	82.50	84.00	84.50	82.90
ṁ [kg/s]	20.78	20.43	19.78	18.84	17.83
M_{max}	1.93	1.69	1.65	1.75	1.84

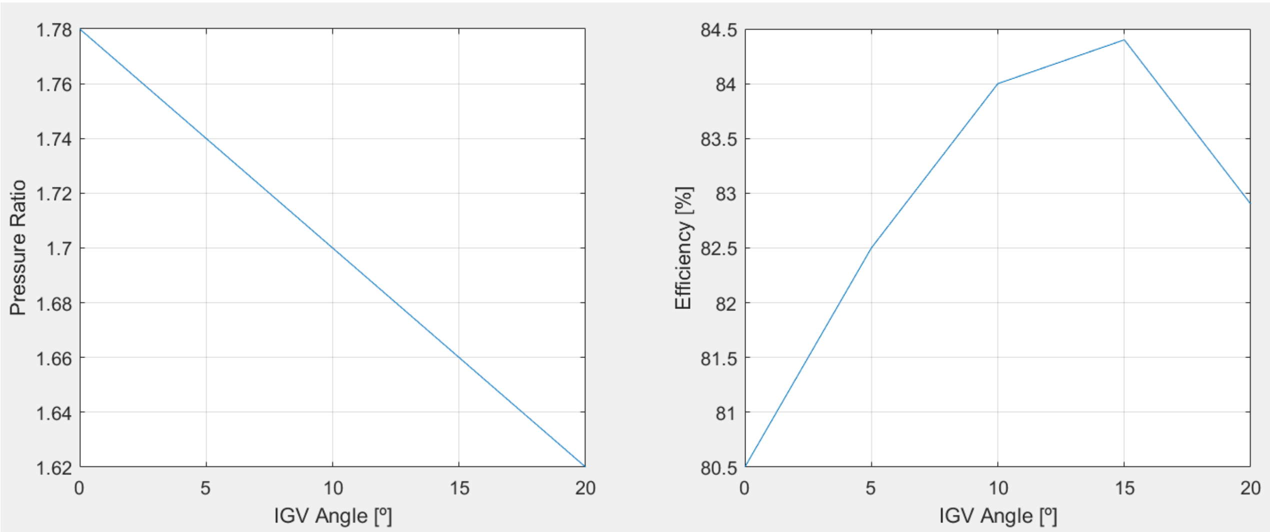

Figure 6. Pressure ratio and efficiency evolution with increase in IGV blades angle.

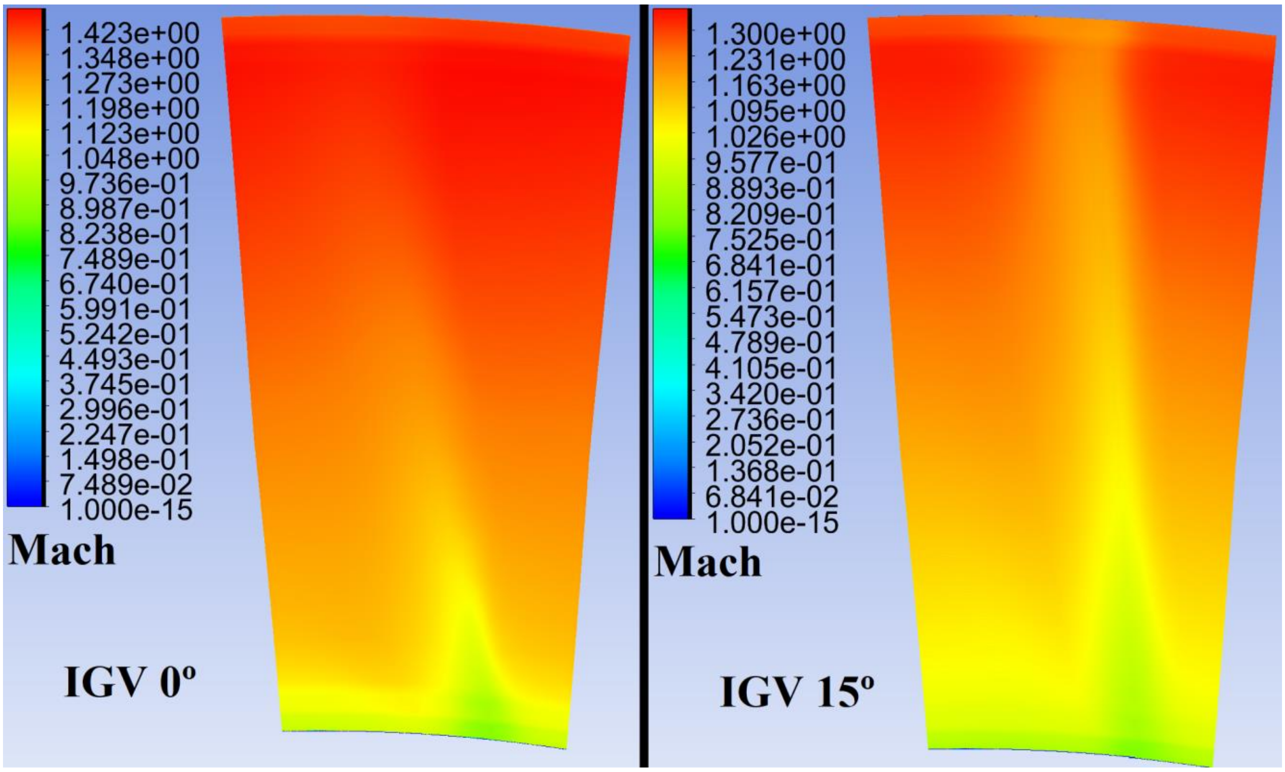

Figure 7. Mach profile at rotor blades inlet at 0º and at the maximum efficiency point.

The results were as expected for a positive pre-swirl, starting with a decrease in the pressure ratio as the swirl angle increased. Additionally, efficiency showed an increase, peaking at 15° with an efficiency of 84.5%, a 5% increase compared to the base value of 0°. As seen before, the increase in efficiency can be explained by the Mach number. Figure 7 allows us to analyze the reduction in the Mach number field at the IGV-rotor interface, from the base condition to the condition of maximum efficiency. Similar behavior can be observed for the maximum global Mach number, occurring near the rotor leading edge, closer to the shroud. Furthermore, due to a restriction in the flow passage area, there is a reduction in the mass flow rate of the air, approximately 2 kg/s at the condition of maximum efficiency, which can have an impact depending on the application.

It can be observed that at the IGV-rotor interface, there is a decrease of approximately 11% in the Mach number from the base condition to the maximum efficiency condition, while the global Mach number experiences a decrease of 12%, which confirms the improvement in compressor efficiency. It is also noticeable that the Mach number increases beyond 15°, accompanied by a decrease in efficiency. This can be explained by the formation of vortices on the blade, where the velocity components within the vortex can locally increase the Mach number, as the effect of reducing the resultant relative velocity is mitigated and introduces a new source of losses in the compressor. A representation of the vortex development is shown in Figure 8, where a very sudden intensification of the vortex is observed, coinciding with the decrease in efficiency and increase in Mach number, occurring at angles above 15° where flow separation begins.

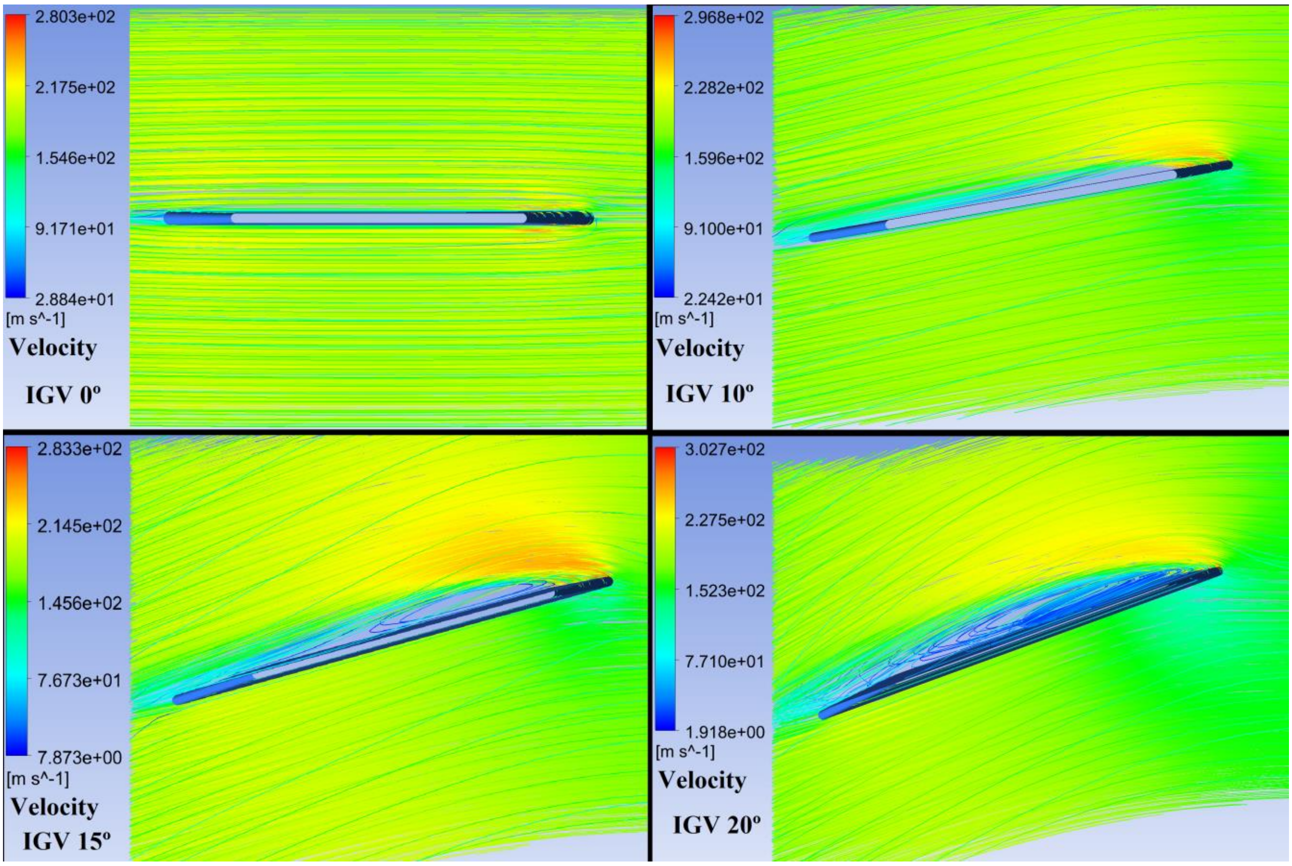

Figure 8. IGV blade vortex development.

The decrease in pressure ratio could be mitigated and efficiency could be optimized through an optimization study of the IGV blade shape, which is not ideal in this case. Additionally, if the number of IGV blades were increased, the vortex formation could be delayed as the flow would be better aligned with the blades due to their mutual influence. However, with this change, the reduction in compression could be even greater, which may not be desirable depending on the application. Nevertheless, as this study is not aimed at implementation but rather for didactic purposes of observing the effects on the compressor's operating parameters, the chosen geometry fulfills its role effectively.

4. CONCLUSION

Based on the obtained results, it was possible to study the parameters of an axial compressor in the presence of an IGV, and the expected behavior from theory was reproduced. Essentially, for a positive pre-swirl, there was a reduction in the pressure ratio and mass flow with an increase in efficiency. At the point of maximum efficiency, there was a 5% increase in efficiency. However, due to the reduction in pressure ratio and mass flow rate, its application may be compromised, and the utilization of an IGV set depends on the specific application. Additionally, since IGVs have operational limits, especially in non-optimized blades like in this case, intense vortices begin to occur at higher angles, which ultimately affects the overall equipment performance. Therefore, any structure designed with this purpose should consider these effects and mitigate the disadvantages by optimizing the shape of the IGV blades.

The results of this study allowed for a deeper understanding of axial compressors operation, which is found in various applications and can be modified and optimized. Furthermore, the main objective of this work was to study a new issue and new CFD models, which were successfully achieved as the model worked and was validated against experimental results.

5. ACKNOWLEDGEMENTS

The authors would like to express their gratitude to the Institute for Technological Research for permitting access to the software necessary to the development of this work.

6. REFERENCES

Boyce, M., 2012. Gas Turbine Engineering Handbook. 4ª ed., Elsevier, Waltham.

Daroukh, M., Moreau, S., Gourdain, N., Boussuge, J.F., Sensiau, C., 2017. Effect of Distortion on Turbofan Tonal Noise at Cutback with Hybrid Methods. International Journal of Turbomachinery Propulsion and Power.

Farokhi, S., 2014. Aircraft Propulsion. 2ª ed., Wiley.

Frohnapfel, D.J., 2019. Methodology Development and Investigation of Turbofan Engine Response to Simultaneous Inlet Total Pressure and Swirl Distortion. Doctorate Thesis, Virginia Polytechnic Institute and State University.

Frank, R.G., Wacker, C., Niehuis, R., 2021. Loss Characterization of a Conventional Variable Inlet Guide Vanes. 14th European Conference on Turbomachinery, Fluid Dynamics and Thermodynamics.

Fredrick, N. J., 2010. Investigation of the Effects of Inlet Swirl on Compressor Performance and Operability Using a Modified Parallel Compressor Model. Master's Thesis, University of Tennessee.

Kozak, J.D., 2000. Investigation of Inlet Guide Vane Wakes in a F109 Turbofan Engine with and without Flow Control. Doctorate Thesis, Virginia Polytechnic Institute and State University.

Matteo, P., 2013. Structural and Fluid-Dynamic Analysis of an Axial Compressor with Adjustable Inlet Guide Vanes. Università Degli Studi Di Padova.

NASA, 1978. Design and Overall Performance of Four Highly Loaded, High-Speed Inlet Stages for an Advanced High-Pressure-Ratio Core Compressor. NASA Technical Paper 1337.

Simões, M.R., Montojos, B.G., Moura, N.R., Sujian, J.S., 2009. Validation of Turbulence Models for Simulation of Axial Flow Compressor. 20th International Congress of Mechanical Engineering.

Singh, P., Kaurase, K.P., 2016. Study of VIGV in Axial-Flow Compressor with Special Emphasis on Climate Change. International journal of Engineering, Science and Computing, vol. 6, no. 6.

Vlady, T.R., Yatsko, A.J., Mavris, D.N., 2021. Effect of Variable Inlet Guide Vanes (VIGV) on a Small Gas Turbine Engine. American Institute of Aeronautics and Astronautics SciTech 2021 Forum.

7. RESPONSIBILITY NOTICE

The authors are solely responsible for the printed material included in this paper.